Coherent population trapping resonances in Cs atoms excited by elliptically polarized light

K. Nasyrov
Institute of Automation and Electrometry, Novosibirsk, Russia

S. Cartaleva* and N. Petrov
Institute of Electronics, Bulgarian Academy of Science, boulevard Tzarigradsko Shosse 72, 1784 Sofia, Bulgaria

V. Biancalana, Y. Dancheva, E. Mariotti, and L. Moi
Department of Physics, University of Siena, Via Roma 56, 53100 Siena, Italy
(Received 15 August 2005; published 25 July 2006)

Coherent population trapping (CPT) resonances study in Hanle configuration is reported for different polarizations of the exciting light field, on the D_2 line of Cs atoms. While for linear/circular polarization dip/peak in the fluorescence is registered, in case of elliptical polarization, a complex shape resonance is evidenced experimentally, whose profile strongly depends on the ellipticity of polarization. A theoretical model is proposed and developed, which includes the influence on the resonance of polarization ellipticity, transverse magnetic field, and spatial intensity profile of the laser beam. Good agreement is found between the theoretical and experimental results. The reported results allow one to accomplish more profound than in previous research analysis of the CPT resonances behavior pointing out their sensitivity to the light polarization and power as well as to transverse magnetic fields. The presented study is of general importance for the wide application of the coherent resonances in high resolution spectroscopy and precise measurements. The purity of linear/circular polarization of the light needed in different applications can be estimated implementing the proposed model.

DOI: 10.1103/PhysRevA.74.013811 PACS number(s): 42.50.Gy, 32.80.Bx, 32.70.Jz

I. INTRODUCTION

Degenerate two-level systems provide many possibilities for investigation of coherent effects arising from the interaction of laser light with an atomic ensemble. In the so called Hanle configuration, subnatural width resonances are observed when a magnetic field is scanned around zero value, due to the orientation/alignment of atoms induced by the light field and its destruction by applied magnetic field [1,2]. Zeeman optical pumping modified by the magnetic field allows for observation of both reduced absorption (dark) [1] and enhanced absorption (bright) [3] magneto-optical resonances in atomic medium, depending on whether $F_g \rightarrow F_e \leqslant F_g$ or $F_g \rightarrow F_e > F_g$ transitions are excited. Here F_g and F_e denote the quantum numbers of the total angular momenta of the ground and excited states, respectively. Excitation with pure linearly or circularly polarized light produces a single dark or bright resonance in the fluorescence when the magnetic field is swept around zero [4]. Both types of resonances have been previously investigated mainly with linearly or circularly polarized light. However, in the real experimental setups and in practical devices the pure linear/circular polarization is not usually realized and it is important to clarify the influence of the polarization ellipticity on the resonance behavior. Due to the wide application of coherent resonances in atomic clocks [5], in precise magnetic field measurement [6], in slowing down of the light [7], and in other fields, an investigation of the influence of the light polarization on the resonance parameters is of general interest. In fact, the resonance shape, width, and contrast determine the ultimate accuracy of the practical devices. A profound understanding of the influence of light polarization ellipticity on atomic spectra is important for both the construction of precision devices and also for high resolution spectroscopy development. In Ref. [8], the atomic angular-momentum distribution created by optical pumping with elliptically polarized light has been considered. Great attention has been paid to atomic motion through light with gradients of polarization, in order to perform atom cooling below the so called Doppler limit [9,10]. Light polarization effects have also been of interest in the study of nonlinear polarization spectroscopy [11] and atom-light interactions [12], although these studies have been carried out in the absence of a magnetic field. Moreover, in the last work a theory was developed related only to atomic energy levels with small value of the angular momenta. A subject closely related to the magneto-optical resonances is the nonlinear self-rotation of polarization that has been studied theoretically and experimentally in transmission spectra of alkali atoms [13]. In that case a discrepancy between theoretical and experimental spectra has been obtained. The discrepancy has been interpreted in terms of nonuniform transverse power distribution in the laser beam, not taken into account in the calculations. Nonlinear magneto-optical rotation of elliptically polarized light interacting with Rb atoms has been studied [14] and it has been shown that for the simple three-level Λ system, the rotation does not depend on the light ellipticity. For more complicated N- and M-level scheme, however, the ellipticity dependent rotation has been evidenced. It should be pointed out that only the magnetic field parallel to the laser beam has been considered there.

In the present paper we report on the effect of elliptically polarized light excitation on coherent population trapping

*Electronic address: stefka-c@ie.bas.bg

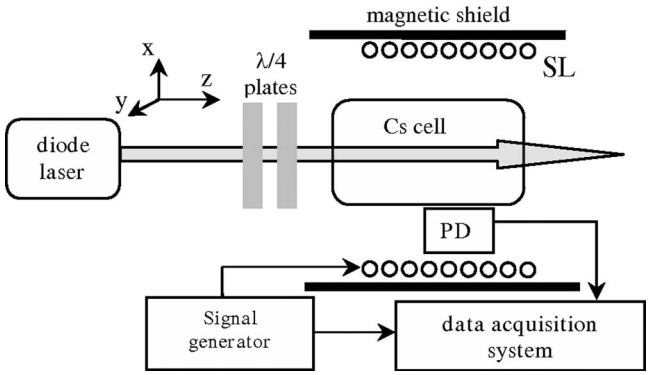

FIG. 1. Experimental setup.

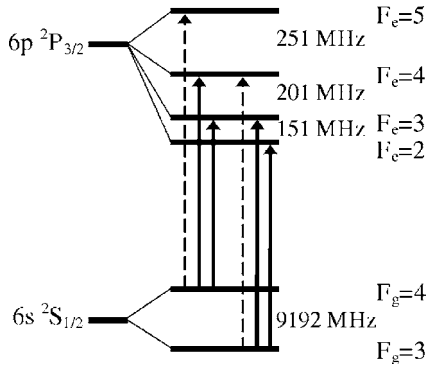

FIG. 2. Energy-level diagram for the D_2 line of Cs. $F_g \rightarrow F_e \leqslant F_g$ transitions (solid line) are distinguished from $F_g \rightarrow F_e > F_g$ transitions (dashed line).

(CPT) resonances in a Hanle configuration, taking into account also transverse components of the magnetic field. Laser excitation with different polarization ellipticities is applied to the D_2 line hyperfine (hf) transitions of Cs atoms. A complex shape of the fluorescence profile is experimentally observed: it consists of a "broad" dip containing a superimposed narrow peak. This shape strongly depends on the ellipticity of polarization, as well as on the magnetic field direction. A theoretical model is proposed and developed, which includes the influence on the resonance of (i) the polarization ellipticity, (ii) the transverse magnetic field components, and (iii) the spatial intensity profile of the laser beam. Our study has shown that the origin of the complexity of the resonance profile is related to the transverse magnetic field. In this way, the experiment stimulated a theoretical model development involving an additional magnetic field of orthogonal to the laser beam orientation that can be expanded to arbitrary field orientation. The theoretical study has shown that, beside the resonance shape dependence on polarization, its profile is strongly influenced by the irradiating power density. It turns out that the involvement in the theoretical model of the nonuniform transverse intensity distribution in the laser beam is of principal importance for the existence of the narrow peak in the fluorescence at high light power.

Good agreement is found between the theoretical and experimental results.

II. EXPERIMENTAL SET UP AND RESONANCE PROFILE

The scheme of the experimental setup is presented in Fig. 1. A collimated beam emitted by a diode laser propagates in the z direction of the laboratory coordinate system. The laser light polarization is adjusted by means of two quarter-wave plates. The ratio of the light intensity values along the x and y axes (I_x, I_y) is measured using a polarizing beam splitter and a power meter (not shown in Fig. 1).

The laser light, with beam radius 0.15 cm, irradiates Cs atoms confined in a cell placed in a solenoid SL producing a longitudinal magnetic field B_z along the z axis. The solenoid is supplied by a signal generator and the magnetic field is periodically scanned around $B_z=0$ value. In the main part of the experiment the cell and the solenoid are situated inside a single μ-metal cylinder for shielding against laboratory stray magnetic fields. This nonperfect shielding results in a residual magnetic field of few tens of mG inside the μ-metal cylinder. In order to clarify the influence of an orthogonal to the laser beam magnetic field $B_\perp$ on the resonance profile (see the end of Sec. IV), a second significantly better shielding system was used providing less than a 0.1 mG internal transverse magnetic field. Additionally to the longitudinal field, a well-controlled transverse magnetic field can be applied by coils situated in the shield (not shown in Fig. 1). The D_2 line fluorescence is collected by means of a photodiode and the signal is processed via a data acquisition system. The fluorescence dependence on magnetic field B_z exhibits a narrow feature when B_z is scanned around $B_z=0$. The feature profile is investigated for different polarizations of the irradiating light.

The Cs energy level diagram related to the D_2 line, with the hf transitions, is presented in Fig. 2. It is well known that the D_2 line of Cs consists of two groups of transitions—starting from the two ground-state hf levels with quantum numbers: $F_g=3$ and $F_g=4$. Due to the smaller frequency separation between the excited-state hf levels compared to the Doppler broadening, each set of transitions forms a single fluorescence line. For each of these two lines, as previously shown [2,4,15], the sign (peak or dip) of the resonances obtained through magnetic field scanning around zero is determined by the closed transitions. Detailed experimental study [15] of resonance sign dependence on the exciting light detuning has shown that there is no resonance sign reversal along the fluorescence profile although the two types (Fig. 2) of hf transitions (responsible for dark or bright resonance) form the fluorescence line. As the experiment has been done in dilute Cs vapor (thus avoiding velocity changing collisions between Cs atoms), the three hf transitions that form a fluorescence line are excited independently, each one at a different velocity class of atoms. Under these conditions the open transitions are depleted due to the hf optical pumping and do not play measurable role in the formation of the resonance. At the same time, the closed transitions that do not suffer hf optical pumping determine the sign of the magneto-optical resonance. Therefore, for the $F_g=3$ fluorescence line, the resonance sign is determined by the $F_g=3 \rightarrow F_e=2$ transition and for the $F_g=4$ fluorescence line—by

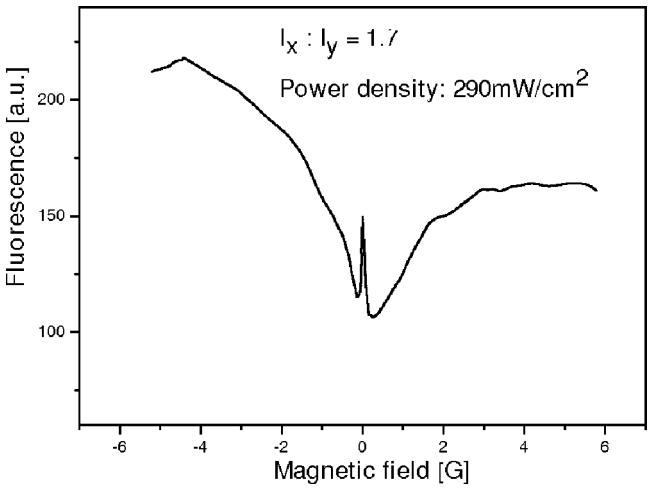

FIG. 3. Resonance profile observed in case of excitation with elliptically polarized light.

the $F_g=4\rightarrow F_e=5$ transition. With linearly polarized light (electrical vector on the x,y plane and $B_z=0$) tuned to the $F_g\rightarrow F_e=F_g-1$ transition, the atoms are optically pumped to the $m_{Fg}=\pm F_g$ Zeeman sublevels noninteracting with the light field (in a system of coordinates with quantization axis along the electrical field vector), while when the laser is tuned to the $F_g\rightarrow F_e=F_g+1$ transition, the atoms are optically pumped to the sublevels most strongly coupled to the excited state (i.e., $m_{Fg}=0,\pm 1$). When $B_z\neq 0$ is applied, the populations of these noncoupled and strongly coupled states are depleted by magnetic transitions. In this way, for the first type transition, a dip (dark resonance) [1] in the fluorescence is observed, while for the second one—a narrow peak (bright resonance) [15,16] occurs. In this paper we consider only the hf transitions starting from $F_g=3$.

The CPT resonance in fluorescence, obtained by scanning the magnetic field B_z around $B_z=0$, has been investigated for different polarizations of the irradiating light. During all experiments the laser frequency is tuned to the maximum of the fluorescence line. With linear or circular light polarization, a single dip or peak in the fluorescence is observed. In case of elliptical polarization, the resonance profile exhibits instead a complex shape, as shown in Fig. 3 for elliptically polarized light with ratio of the intensities $I_x:I_y=1.7$. It can be seen that a narrow peak is superimposed on a broad dip in the fluorescence profile.

III. THEORETICAL DESCRIPTION

In order to analyze the CPT resonance behavior for atom excitation by elliptically polarized light, the following theoretical model is proposed. It is well-known [17] that, for $B=0$ and $F_g\rightarrow F_e=F_g-1$ transition, the light of arbitrary polarization prepares the atomic system into a so called "dark state," in which it does not interact with the light field.

In a system of coordinates with the z axis aligned to the wave vector of the light, the elliptical polarization of the light wave can be represented as a sum of two circular components:

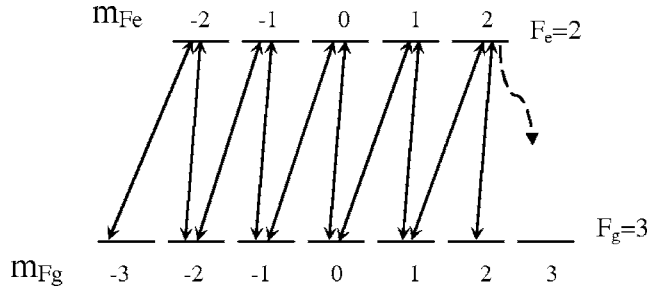

FIG. 4. Scheme of the optical transitions within the $F_g=3\rightarrow F_e=2$ configuration, in the rotated system of coordinates.

$$\mathbf{E}=\mathbf{E}_{+1}+\mathbf{E}_{-1}. \tag{1}$$

However, as introduced and discussed in detail in Refs. [18,19], a natural (x',y',z') coordinate frame can be chosen, in which the polarization ellipse can be represented as a sum of one circular component in the new x',y' plane and a linear component along the new z' axis:

$$\mathbf{E}=\mathbf{E}'_{+1}+\mathbf{E}'_{0}. \tag{2}$$

The y' axis coincides with the y axis and the two frames are connected by a rotation angle Θ around the y axis determined as followed:

$$\cos\Theta=\frac{|E_{-1}|-|E_{+1}|}{|E_{-1}|+|E_{+1}|}=\sqrt{\frac{I_y}{I_x}}. \tag{3}$$

The axis z' lies in the plane defined by the axis z and the longer axis of the polarization ellipse (the angle between the axes z and z' being Θ). Here, it is assumed that the longer axis of the polarization ellipse is along the axis x, so that $I_x\geqslant I_y$.

In the (rotated) coordinate system, using the z' axis as a quantization axis, the optical transitions between Zeeman sublevels within the $F_g=3\rightarrow F_e=2$ hf transition, driven by the light field described by Eq. (2), are shown in Fig. 4. It can be seen that only one state, namely $m_{Fg}=F_g$, does not interact with the light. As a result of the optical transitions and spontaneous decay of the excited states, all atoms are pumped into the $m_{Fg}=F_g$ state, thus ceasing to interact with the light. In other words, due to the optical orientation, all atoms are pumped into the dark state.

However, if a constant magnetic field $H_\perp$ is applied orthogonally to the atomic orientation (with respect to the rotated coordinate system), the m_{Fg} sublevels will evolve one into the other and their populations will be mixed with a rate proportional to the magnetic field value. Thus, atoms accumulated on the $m_{Fg}=F_g$ sublevel will be transferred into the $m_{Fg}=F_g-1$ state, from where they can again be excited by the light into the $m_{Fe}=F_e$ state, which spontaneously decays to $m_{Fg}=F_g$, F_g-1, F_g-2. For the hf transition depicted in Fig. 4, most of the atoms in the $m_{Fe}=F_e$ state decay into the $m_{Fg}=F_g$, F_g-1, and not more than 5% of all atoms decay into the $m_{Fg}=F_g-2$ state because of the unfavorable Clebsch-Gordon coefficients.

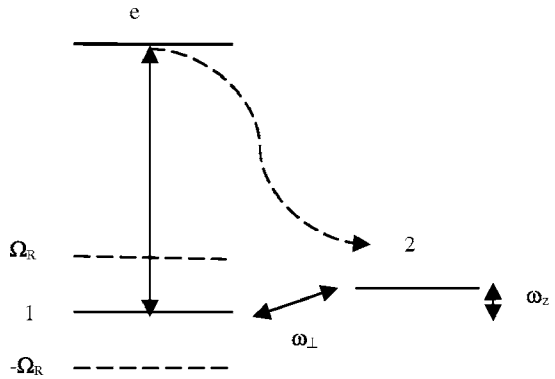

FIG. 5. Three-level system, equivalent to the system of Fig. 4 in the presence of small orthogonal magnetic field.

Thus, even in the presence of a small magnetic field mixing the m_{Fg} sublevels, most of the atoms will be accumulated in the $m_{Fg}=F_g$, F_g-1 states. For this reason, without strong sacrifice in the accuracy, the full $F_g=3-F_e=2$ system can be approximated as a three-level system.

A quantitative criterion for the applicability of this approximation is given by the following condition:

$$\frac{\Omega_R^2}{\Gamma} > \omega_\perp, \tag{4}$$

where $\omega_\perp=\mu_0 g\sqrt{F_g/2}H_\perp/\hbar$ is the evolution rate of the $m_{Fg}=F_g$, F_g-1 sublevel population caused by the magnetic field $H_\perp$, Ω_R is the Rabi frequency of the optical transition $m_{Fg}=F_g-1\rightarrow m_{Fe}=F_e$, and 2Γ is the spontaneous decay rate of the excited state. Condition (4) means that the optical depletion of the state $m_{Fg}=F_g-1$ is faster than its repopulation through the magnetic transitions. Thus, instead of the system of Fig. 4, the three-level system shown in Fig. 5 will be considered.

The equations for the density matrix elements describing such three-level quantum system, are the following:

$$\frac{\partial}{\partial t}\rho_{e,e}+2\Gamma\rho_{e,e}+i\Omega_R(\rho_{1,e}-\rho_{e,1})=0,$$

$$\frac{\partial}{\partial t}\rho_{e,1}+(\Gamma-i\Omega)\rho_{e,1}+i\omega_{+1}^*\rho_{e,2}+i\Omega_R(\rho_{1,1}-\rho_{e,e})=0,$$

$$\frac{\partial}{\partial t}\rho_{e,2}+(\Gamma-i\Omega-i\omega_z)\rho_{e,2}+i\omega_{+1}\rho_{e,1}+i\Omega_R\rho_{1,2}=0,$$

$$\frac{\partial}{\partial t}\rho_{2,2}-i\omega_{+1}^*\rho_{1,2}+i\omega_{+1}\rho_{2,1}=\alpha_2 2\Gamma\rho_{e,e},$$

$$\frac{\partial}{\partial t}\rho_{1,2}-i\omega_z\rho_{1,2}+i\omega_{+1}(\rho_{1,1}-\rho_{2,2})+i\Omega_R\rho_{e,2}=0,$$

$$\frac{\partial}{\partial t}\rho_{1,1}-i\omega_{+1}\rho_{2,1}+i\omega_{+1}^*\rho_{1,2}+i\Omega_R(\rho_{e,1}-\rho_{1,e})=\alpha_1 2\Gamma\rho_{e,e}. \tag{5}$$

Here $\omega_z=\mu_0 g H_z$ is the Zeeman splitting of the magnetic sublevels due to the component of the magnetic field vector which lies along the z' axis, α_1 and α_2 are the branching ratios of the decay of the excited state into the ground states 1 and 2 of the three-level system ($\alpha_1+\alpha_2=1$, $\alpha_2=0.714$), and Ω is the optical detuning of the light frequency from the frequency of the transition $1\rightarrow e$.

From the system of equations (5) the particle conservation law can be obtained:

$$\frac{\partial}{\partial t}(\rho_{1,1}+\rho_{2,2}+\rho_{e,e})=0.$$

The following normalization will be used:

$$\rho_{1,1}+\rho_{2,2}+\rho_{e,e}=1. \tag{6}$$

Equation (6) can be used to replace any of the equations from the system (5).

The stationary-state solution of the system (5) can be obtained:

$$\rho_{e,e}=\frac{\Omega_R^2}{2\alpha_1\Omega_R^2+2\Gamma^2+2\omega_\perp^2+\Omega^2+(\Omega+\omega_z)^2+\alpha_2(3\omega_z^2+4\omega_z\Omega)+\alpha_2\dfrac{\Gamma^2\omega_z^2+[\Omega_R^2-\omega_z(\Omega+\omega_z)]^2}{\omega_\perp^2}}, \tag{7}$$

where $\omega_\perp=|\omega_{+1}|=\mu_0 g\sqrt{F_g/2}H_\perp/\hbar$, and $H_\perp=\sqrt{H_x^2+H_y^2}$.

Let us now consider the fluorescence behavior. The fluorescence intensity is proportional to the population $\rho_{e,e}$ of the excited state. The most interesting and important condition for applications is the weak orthogonal magnetic field $\omega_\perp<\Gamma,\Omega_R$. In this case, and at exact resonance ($\Omega=0$), Eq. (7) is simplified to the form:

$$\rho_{e,e}=\frac{\Omega_R^2\omega_\perp^2}{\alpha_2[\omega_z^4+(\Gamma^2-2\Omega_R^2)\omega_z^2+\Omega_R^4]+\omega_\perp^2[2\alpha_1\Omega_R^2+2\Gamma^2+\omega_z^2(1+3\alpha_2)]}. \tag{8}$$

As the studied experimental resonance is observed in the fluorescence dependence on the longitudinal magnetic field H_z (that means on the Zeeman splitting frequency ω_z), we have performed the corresponding analysis of Eq. (8). This analysis shows that two cases should be considered separately: weak electromagnetic (e.m.) field ($\Omega_R < \Gamma/\sqrt{2}$) and strong e.m. field ($\Omega_R > \Gamma/\sqrt{2}$). In weak fields, the dependence of $\rho_{e,e}$ on ω_z gives a single peak centered at $\omega_z=0$, whose width is:

$$\Delta\omega_z = \sqrt{\frac{\Omega_R^4}{\Gamma^2} + \frac{2\omega_\perp^2}{\alpha_2}},$$

and whose amplitude is expressed by:

$$\rho_{e,e} = \frac{\omega_\perp^2 \Omega_R^2}{\alpha_2 \Omega_R^4 + \omega_\perp^2 (2\Gamma^2 + 2\alpha_1 \Omega_R^2)}. \tag{9}$$

In a strong e.m. field this peak is split into two peaks, separated by a dip and centered at $\omega_z = \pm\sqrt{\Omega_R^2 + \Gamma^2/2}$. The two peaks amplitude is determined by:

$$\rho_{e,e} = \frac{\Omega_R^2 \omega_\perp^2}{\alpha_2 \Gamma^2 (\Omega_R^2 - \Gamma^2/4)}. \tag{10}$$

The population at the center of the dip, situated between the two peaks, is again given by Eq. (9) which determines the peak amplitude at the weak light field. In the limit of high light intensity $\Omega_R^2 > \Gamma^2$, from Eq. (10) follows that the maximum of the population does not depend on the light intensity any more.

The underlying physical process leading to the splitting of the peak in two peaks by increasing the light intensity can be explained on the basis of Fig. 5. Under the influence of the light resonant with the $1 \rightarrow e$ transition, the level 1 (and also level e) are split into two quasilevels, situated on the two sides of the unperturbed level and separated by the Rabi frequency. Similarly to Autler-Townes effect, the transition due to magnetic mixing of the levels 1 and 2 is most probable when the energy of the state 2 coincides with one of the quasilevels. When the Rabi frequency is smaller than the transition linewidth, the two quasilevels are not resolved and there is a single peak centered at $\omega_z=0$. However, for $\Omega_R^2 > \Gamma^2$, two peaks are registered, separated by a dip, whose width is Ω_R. It should be pointed out that the single peak centered at $H_z=0$ (weak light fields) and the two peaks that occur for strong light fields are due to the constant magnetic field $H_\perp$ applied orthogonally to the atomic orientation [see Eqs. (9) and (10)]. Hence, the introduction in the presented model of an additional magnetic field component orthogonal to the scanned longitudinal magnetic field is of significant importance for the adequate analysis of the magneto-optical resonances.

In the present analysis the scanned magnetic field was supposed to be along the axis z' of the rotated coordinate system, where the electrical field of the light is described by Eq. (2). In the experiment, the magnetic field is scanned along the axis z of the laboratory coordinate system. In order to take this into account, in Eq. (8) the following substitution should be introduced:

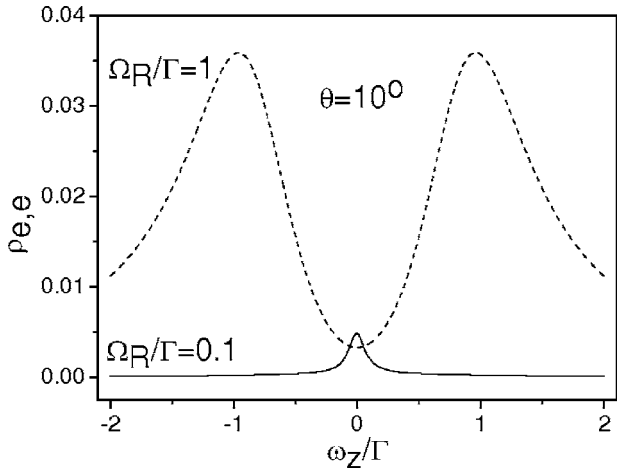

FIG. 6. Dependence of the excited-state population on the scanned magnetic field, for the cases of strong (dashed line) and weak (solid line) optical fields: $\Theta=10°$, $\omega_\perp/\Gamma=0.05$.

$$\omega_\perp^2 = \omega_{\perp 0}^2 + \varpi_z^2 \sin^2\Theta,$$

$$\omega_z^2 = \varpi_z^2 \cos^2\Theta, \tag{11}$$

where ϖ_z is the Zeeman frequency for magnetic field along the z axis of the laboratory coordinate system. The condition for the angle Θ, and therefore the ellipticity at which it is possible to observe the central peak, can be obtained in a simple way. In order to observe a peak at $\varpi_z=0$, the following condition must be satisfied for the $\rho_{e,e}$ dependence on ϖ_z:

$$\frac{d\rho_{e,e}}{d\varpi_z^2} < 0.$$

Calculation of this derivative at $\varpi_z=0$ leads to:

$$\tan\Theta < \frac{\omega_{\perp 0}\Gamma}{\Omega_R^2\sqrt{\alpha_2}}. \tag{12}$$

Thus, the ellipticity at which there is a central peak depends on the ratio of the optical depletion rate of level 1 and the rate of its repopulation through mixing by the magnetic field. When these two rates are of the same order, the central peak can be observed with polarization rather different from circular.

As an example, the dependence of the excited state population on ω_z, based on the analysis of Eqs. (8) and (11), is presented in Fig. 6, for the cases of strong and weak optical field (at $\Theta=10°$). Thus, in the present work the proposed simplified theoretical analysis shows that for weak optical fields, a narrow peak in the excited-state population, centered at $\omega_z=0$ is expected. For the same ellipticity of the light polarization, due to the peak splitting in strong light fields, a broad dip is centered at $\omega_z=0$.

Taking into consideration the experimental conditions, the fluorescence is calculated for elliptically polarized light. In Fig. 7, the calculated fluorescence dependence on H_z is shown, for the Cs $F_g=3 \rightarrow F_e=2$ transition at different laser power levels and ellipticity $I_x:I_y=1.7$. These spectra were

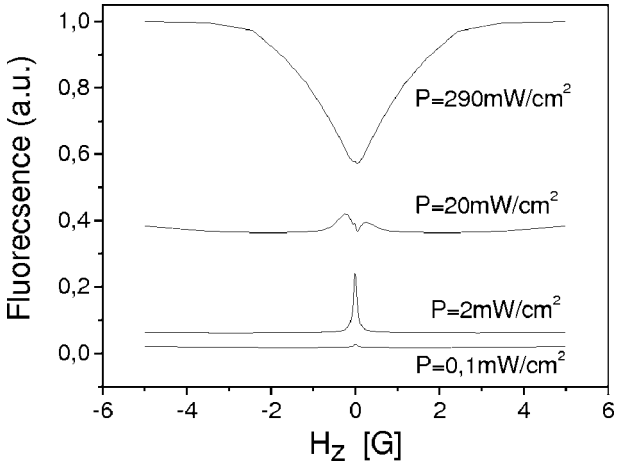

FIG. 7. Calculated fluorescence profiles at four different laser powers. $I_x:I_y=1.7$.

obtained by solving the optical Bloch equations (OBE) for the level system corresponding to the Cs D_2 line. Averaging over the atomic velocities was performed both for the atoms crossing the laser beam and for those moving along it. The methodology of these calculations was presented in an earlier work [15]. From Fig. 7 it can be seen that the result of the numerical OBE solution is in agreement with that of the simplified analytical model described above. Namely, at elliptical polarization when increasing the light intensity, the resonance starts as a narrow peak and passing through a complex profile turns into a broad dip. It should be noted that the fluorescence intensity variations with incident light intensity are not large. As can be seen from Fig. 7, resonant light differing in intensity by two orders of magnitude, gives a comparable contribution to the fluorescence.

IV. COMPARISON BETWEEN THEORETICAL AND EXPERIMENTAL RESULTS

First, the developed model was experimentally tested for the case of atom irradiation by linearly polarized light. In this case, as shown in [1], a dip in the fluorescence dependence on the scanned around zero value magnetic field is observed which is attributed to a coherent superposition of the ground-state Zeeman sublevels by σ^+ and σ^- polarized laser light. An example of the dark resonance experimentally obtained with linear polarization of the light is presented in Fig. 8(a). As can be seen, the shape and the contrast of the experimental profile are in good agreement with those following from the model developed in this work. Note that the experimental results presented in Figs. 8, 9, and 10 have been observed applying the poor single-cylinder shielding (see Sec. II).

The case of circular polarization has been experimentally examined in a previous work by Alzetta *et al.* [4], for Rb. There, a peak in the fluorescence dependence on the magnetic field is evidenced and the following physical processes have been suggested to be responsible for its observation. For circular polarization of the light, the quantization axis can be conveniently taken along the wave vector of the light field. In this case again at zero magnetic field the atomic

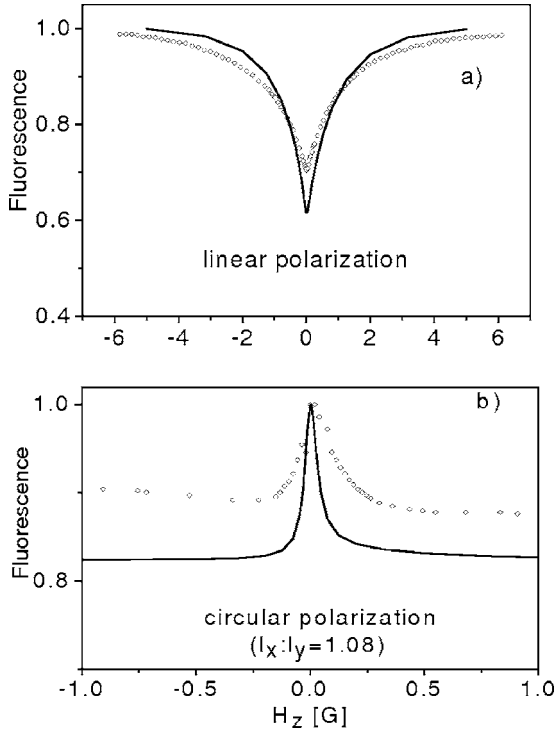

FIG. 8. Theoretical (solid line) and experimental (points) resonance profiles irradiating atoms by linearly (a) and circularly (b) polarized light. Laser power density is of 290 mW/cm^2.

population is accumulated on nonabsorbing Zeeman sublevels—for example, $m_{Fg}=F_g,F_g-1$ for σ^+ polarization. Application of a longitudinal magnetic field (parallel to the quantization axis) does not redistribute the population, so no resonance is expected in this case. However, a small residual transverse magnetic field would play a role around zero lon-

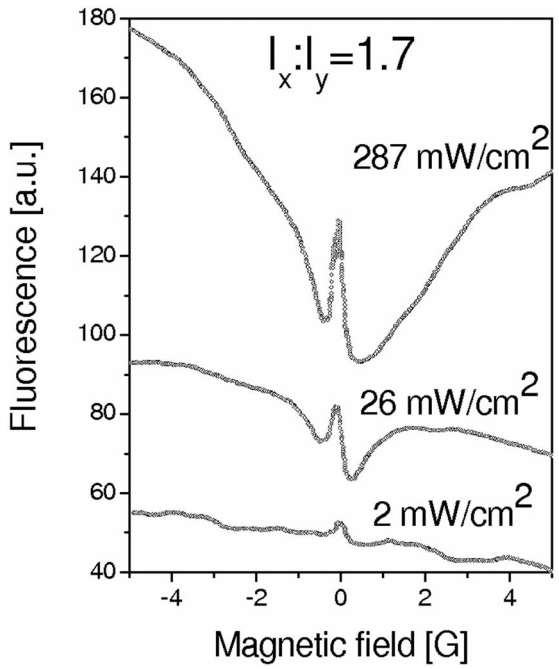

FIG. 9. Resonance profiles for three different light densities.

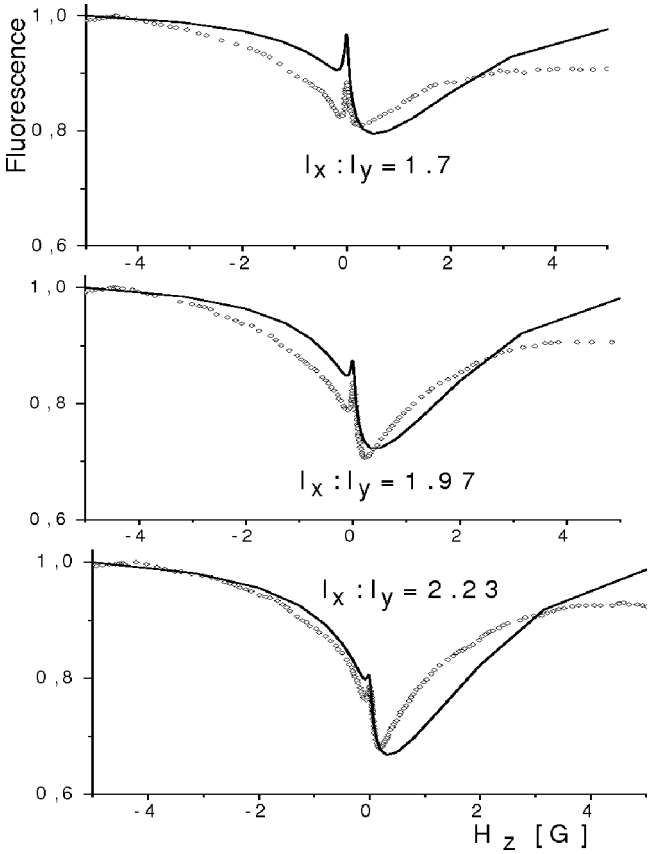

FIG. 10. Theoretical (solid line) and experimental (points) resonance profiles, for different degrees of light polarization ellipticity. Laser power density is of 290 mW/cm^2. In the model $H_\perp$ =0.03 G.

gitudinal magnetic field, thus redistributing the accumulated population among absorbing Zeeman sublevels, leading to increased absorption (fluorescence) around a zero longitudinal magnetic field. Our experimental and theoretical results related to the circular polarization are illustrated in Fig. 8(b). It can be seen that they are in good agreement. In the modeling, $H_\perp$=0.03 G was taken, corresponding to the remaining magnetic field inside the magnetic shield.

Let us consider now the case of elliptical polarization. As shown in Sec. III (Fig. 7), it is expected that the narrow peak will be transformed into a broad dip when the laser intensity is increased. However, our experiment has shown that the narrow peak is observed also at high power density (see Fig. 9). In order to analyze this discrepancy it should be pointed out that in the theoretical model illustrated in Fig. 7, a constant light intensity across the laser beam was assumed. Actually, in the experiment the light intensity is inhomogeneous along the laser beam radius. Due to this fact, the regions in the center of the beam, where the condition for a strong field is met, provide the broad dip in the fluorescence spectrum, while the peripheral regions of the beam, which have weak intensity, create a narrow peak.

Moreover, in the experiment the laser beam is multiply reflected at the cell windows. Each reflection decreases the light intensity more than ten times (the reflection coefficient at one quartz surface is 4%, giving 8% after reflection from

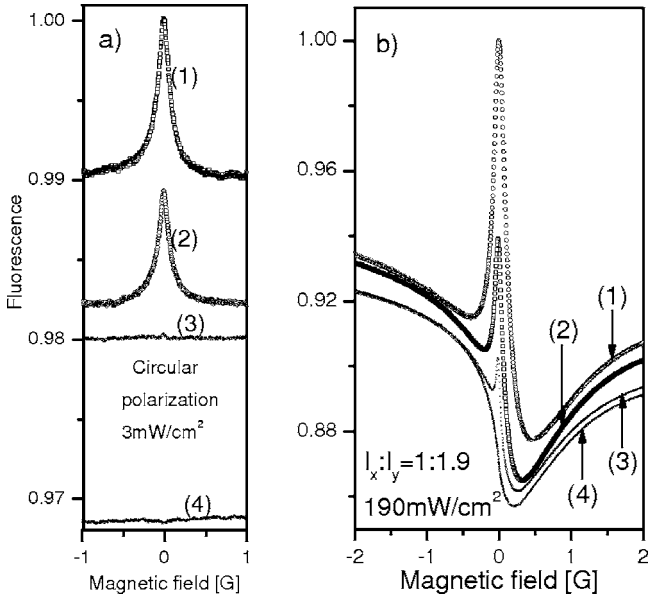

FIG. 11. Dependence of the peak amplitude on the value of the orthogonal to laser beam magnetic field $B_\perp$, for circular [a, $B_\perp$:39.5 mG (1); 31.6 mG (2); 4.1 mG (3); 0.1 mG (4)] and elliptical [b, $B_\perp$:79 mG (1); 47.4 mG (2); 23.7 mG (3); 0.1 mG (4)] polarizations of the light.

the cell window). Therefore, the reflected beams provide an additional contribution to the formation of the narrow central peak. As can be seen from Fig. 9, even at light power density about 290 mW/cm^2, the narrow central peak is very well pronounced, which is not the case in the theoretical model without taking into consideration the existence of low power density areas in the alkali cell (see Fig. 7). Further development of the theoretical analysis has shown that when the Gaussian profile of laser beam intensity and multiple light reflections by the cell windows were taken into consideration the agreement between the experiment and theory became much better. This is illustrated by Fig. 10 where the fluorescence profiles at different ellipticities are shown. There, the light intensity distribution across the laser beam is assumed Gaussian and several reflections on cell windows are taken into account. It can be seen that the light polarization ellipticity strongly influences the complex resonance profile. The amplitude of the peak increases when the ellipticity of the polarization approaches circular. At the same time, the dip becomes less pronounced. Note that at high laser power density, the transverse laser intensity distribution also influences the CPT resonance profile prepared by circular polarization [20,21].

In order to demonstrate that the narrow peak in the fluorescence profile is due to the presence of a transverse magnetic field, such a component was significantly reduced by means of more accurately elaborated shielding system. Moreover, additional coils were situated in the shield to provide a controlled transverse magnetic field. Under these conditions the fluorescence profiles are measured in dependence on the longitudinal magnetic field and the result is presented in Fig. 11. As can be seen, in the case of circular polarization of the beam, no peak is registered for $B_\perp \sim 0.1$ mG [Fig.

11(a)] with the accuracy of our experiment. A very small peak is measured at $B_\perp \sim 4.1$ mG and its amplitude increases with transverse magnetic field enhancement. Similar is the situation for the elliptical polarization illustrated in Fig. 11(b). Here also the narrow peak vanishes for $B_\perp \sim 0.1$ mG but at $B_\perp \sim 24$ mG is already well measurable. The peak amplitude strongly depends on the value of $B_\perp$.

The discussion in this section has shown that only for pure linear or circular polarization of the light the CPT resonance profile represents simple dip or peak, respectively. In case of elliptical polarization the resonance exhibits a more complex shape depending not only on the ellipticity of polarization but also on the intensity profile of the laser beam and on the existence of the magnetic field orthogonal to the beam. Hence, in order to perform adequate analysis of the resonances the particular conditions have to be considered carefully in terms of light polarization, magnetic field orientation, and transverse distribution of the light intensity.

V. CONCLUSIONS

CPT resonances in Cs, on the D_2 line, have been studied, obtained in a Hanle configuration by a laser light excitation resonant with the $F_g=3$ fluorescence line and a scanning of the magnetic field parallel to the light propagation direction. The resonances were investigated depending on the polarization of the irradiating light field. In accordance with previous work, for linear polarization dark resonances in the fluorescence are registered, while for circularly polarized light, bright resonances are obtained. The performed study confirms our proposition that the narrow peak in the fluorescence is due to a constant magnetic field orthogonal to the laser beam. For elliptical polarization, a complex shape of the resonance is obtained, namely a narrow peak appears superimposed on a broader dip. When the light polarization approaches the circular one, the peak amplitude increases, while the dip becomes less pronounced. From the developed theoretical model it can be concluded that for the absolute value measurement of the magnetic field orthogonal to the light beam, special care should be taken in order to avoid the reflected beams in the alkali cell and to keep constant the laser power at the beam cross section. The presented study is of significant importance for the wide application of the coherent resonances for precise measurements which are sensitive to resonance parameters. The purity of linear/circular polarization of the light needed in different metrology applications can be estimated implementing the proposed theoretical model. The presented results also allow one to accomplish more profound research analysis of the CPT resonances prepared in a Hanle configuration, underlining their sensitivity to the light polarization to the existence of transverse magnetic field and to the light power distribution in the laser beam.

ACKNOWLEDGMENTS

The authors thank the EC (Grant No. G6RD-CT-2001-00642). The work was partly supported by the collaboration program between the Italian National Research Council and the Bulgarian Academy of Sciences. We acknowledge the contribution of Dr. C. Andreeva at the early stage of this work. S.C. and N.P. also thank the Bulgarian Council for Scientific Research (Grant No. F-1404/04). K.N. thanks the Russian Foundation for Basic Research (Grant No. 04-02-16771) for the partial support of the work.

[1] F. Renzoni, W. Maichen, L. Windholz, and E. Arimondo, Phys. Rev. A **55**, 3710 (1997).
[2] A. V. Papoyan, A. Auzinsh, and K. Bergmann, Eur. Phys. J. D **21**, 63 (2002).
[3] Y. Dancheva, G. Alzetta, S. Cartaleva, M. Taslakov, and C. Andreeva, Opt. Commun. **178**, 103 (2000).
[4] G. Alzetta, S. Cartaleva, Y. Dancheva, C. Andreeva, S. Gozzini, L. Botti, and A. Rossi, J. Opt. B: Quantum Semiclassical Opt. **3**, 181 (2001).
[5] S. Knappe, V. Shah, P. D. D. Schwindt, L. Hollberg, J. Kitching, L.-A. Liew, and J. Moreland, Appl. Phys. Lett. **85**, 1460 (2004).
[6] P. D. D. Schwindt, S. Knappe, V. Shah, L. Hollberg, and J. Kitching, Appl. Phys. Lett. **85**, 6409 (2004).
[7] L. V. Hau, S. E. Harris, Z. Dutton, and C. H. Behroozi, Nature (London) **397**, 594 (1999).
[8] V. Milner and Y. Prior, Phys. Rev. A **59**, R1738 (1999).
[9] P. R. Berman, Phys. Rev. A **43**, 1470 (1991).
[10] G. Nienhuis, P. van der Straten, and S.-Q. Shang, Phys. Rev. A **44**, 462 (1991).
[11] A. M. Akulshin, V. L. Velichansky, M. V. Krasheninnikov, V. A. Sautenkov, V. S. Smirnov, A. M. Tumaikin, and V. I. Yudin, Sov. Phys. JETP **69**, 58 (1989).
[12] O. N. Prudnikov, A. V. Taichenachev, A. M. Tumaikin, V. I. Yudin, and G. Nienhuis, JETP **126**, 1303 (2004).
[13] S. M. Rochester, D. S. Hsiung, D. Budker, R. Y. Chiao, D. F. Kimball, and V. V. Yashchuk, Phys. Rev. A **63**, 043814 (2001).
[14] A. B. Matsko, I. Novikova, M. S. Zubairy, and G. R. Welch, Phys. Rev. A **67**, 043805 (2003).
[15] C. Andreeva, S. Cartaleva, Y. Dancheva, V. Biancalana, A. Burchianti, C. Marinelli, E. Mariotti, L. Moi, and K. Nasyrov, Phys. Rev. A **66**, 012502 (2002).
[16] F. Renzoni, C. Zimmermann, P. Verkerk, and E. Arimondo, J. Opt. B: Quantum Semiclassical Opt. **3**, S7 (2001).
[17] K. A. Nasyrov, Phys. Rev. A **63**, 043406 (2001).
[18] A. Tumaikin and V. Yudin, Zh. Eksp. Teor. Fiz. **98**, 81 (1990) [JETP Lett. **71**, 43 (1990)].
[19] A. V. Taichenachev, A. M. Tumaikin, V. I. Yudin, and G. Nienhuis, Phys. Rev. A **69**, 033410 (2004).
[20] A. V. Taichenachev, A. M. Tumaikin, V. I. Yudin, M. Stahler, R. Wynands, J. Kitching, and L. Hollberg, Phys. Rev. A **69**, 024501 (2004).
[21] F. Levi, A. Godone, J. Vanier, S. Micalizio, and G. Modugno, Eur. Phys. J. D **12**, 53 (2000).